Analytica Chimica Acta 1074 (2019) 142–149

Contents lists available at ScienceDirect

Analytica Chimica Acta

journal homepage: www.elsevier.com/locate/aca

Proximity hybridization-induced on particle DNA walker for ultrasensitive protein detection

Haiying Gan, Jie Wu*, Huangxian Ju

State Key Laboratory of Analytical Chemistry for Life Science, School of Chemistry and Chemical Engineering, Nanjing University, Nanjing, 210023, PR China

HIGHLIGHTS

- Ultrasensitive protein detection is achieved by on particle DNA walker based signal amplification.
- The assay can detect PDGF-BB down to sub-pM level with a concentration range of 4 orders of magnitude.
- The assay can reliably monitor the secretion of PDGF-BB from cancer cells.
- The assay possesses the features of simplicity, high sensitivity, and good selectivity, applicability and extensibility.

GRAPHICAL ABSTRACT

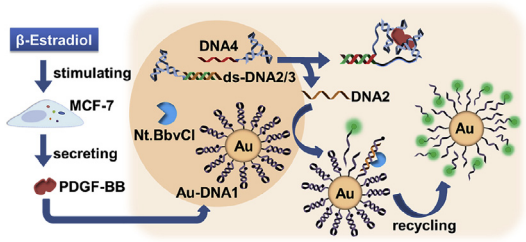

ARTICLE INFO

Article history:
Received 7 March 2019
Received in revised form
18 April 2019
Accepted 5 May 2019
Available online 8 May 2019

Keywords:
Platelet-derived growth factor-BB
Fluorescent assay
DNA walker
Aptamer
Proximity hybridization

ABSTRACT

A simple proximity hybridization-induced on particle DNA walker was designed for ultrasensitive detection of proteins, for example platelet-derived growth factor (PDGF-BB) secreted by cancer cells, in which the DNA walker was activated by specific target binding and powered by an enzymatic cleavage to produce amplified signal. High-density FAM-labeled hairpin oligonucleotides (FAM-DNA1) were functionalized on AuNPs to construct three-dimensional (3D) DNA tracks. The specific binding of PDGF-BB with two aptamer probes (DNA3 and DNA4) led to the proximity hybridization-induced DNA displacement and the free of DNA walker (DNA2) to perform movement on the 3D tracks by an enzymatic cleavage, resulting in the release of massive FAM-DNA1 fragments from the AuNPs and the generation of fluorescent signal. This DNA walker based sensing strategy could detect PDGF-BB in a concentration range of 4 orders of magnitude with a detection limit down to sub-pM level. The practical applicability of the assay was demonstrated by detecting PDGF-BB secreted from MCF-7 cells with satisfactory results. The proposed DNA walker based assay could conveniently detect PDGF-BB with high sensitivity and good accuracy, along with the good extensibility of the assay, showing promise for practical diagnosis.

1. Introduction

Platelet-derived growth factor (PDGF-BB), a significant serum cytokine, involves in processes like embryonic development, wound healing and tissue homeostasis [1]. Because its abnormal expression is related to diseases like atherosclerosis, lung fibrosis and tumors, the detection of PDGF-BB is significant for early clinical diagnosis [2–4]. Antibody-based immunoassays including enzyme-linked immunosorbent assay (ELISA), affinity chromatography and immunohistochemistry are commonly used for PDGF-BB detection in clinic [5,6]. However, because these immunoassay methods

* Corresponding author.
E-mail address: wujie@nju.edu.cn (J. Wu).

https://doi.org/10.1016/j.aca.2019.05.013
0003-2670/

suffer from tedious steps, complicated instrumentation, long assay time and deficient sensitivity, their usage in practical application is challenged [7].

Multiple strategies have been used to design enhanced systems for PDGF-BB detection. Among them, aptamer-based assays are the most attractive. PDGF-BB aptamer is a DNA three-way helix junction and shows high specific binding affinity to PDGF-B chain [8]. By combining the target-induced conformation rearrangement of aptamer with fluorescence energy transfer, electron transfer, and nanoparticle aggregation, a variety of fluorescent [9–11], electrochemical [12], electroluminescent [13], colorimetric [14,15] and chemiluminescent [16] methods have been developed for fast and simple detection of PDGF-BB. However, as the PDGF-BB secreted from cancer cells is normally at low abundance in human serum, the development of assays with high sensitivity is still in urgent need.

The proximity binding-based assay (PDA) which can transform the binding events between protein and pairs of affinity reagents into DNA assemblies has been considered as one of the most efficient protein methods due to the simplicity and variousness of DNA assembly [17,18]. Because the DNA assembly can carry on signal amplifications conveniently by polymerase chain reaction [19,20], exonuclease/endonuclease-mediated cycle amplification [21], hybridization chain reaction [22], and catalytic hairpin assembly [23,24], the PDAs normally show high sensitivity for protein detection. Recently, by combining the proximity binding with the three-dimensional (3D) DNA nanomachines/walkers, the sensing performances of PDA have been further improved. The 3D DNA nanomachines/walkers use high-density oligonucleotides functionalized on nanoparticle surfaces as tracks [25–29], and can be powered by strand displacement [30,31] and enzyme-meditated hydrolysis [32,33]. Due to the high local concentration of DNA tracks, the DNA nanomachines/walkers move quickly on the 3D surfaces to circularly generate signal for sensitive protein detection in vitro [34,35] and in vivo [36]. For example, different kinds of swing arm-based 3D DNA machines have been designed to develop efficient PDA for PDGF detection [25,37]. Although these methods could realize the detection of PDGF at pM level, they may suffer from the preparation of double-functional Au nanoparticles (AuNPs) with precise proportion of DNA tracks and affinity ligands. In addition, affinity binding of protein on the AuNP surface may also bring large steric hindrance and affect the motion area of DNA nanomachines/walkers.

In this work, a proximity hybridization-induced on particle DNA walker was designed for simple and ultrasensitive detection of PDGF-BB. The specific recognition of PDGF-BB with two aptamer probes induced a DNA strand displacement [24] to activate the DNA walker which could walk on the 3D DNA track via nicking endonuclease-meditated hydrolysis [25], resulting in the circular generation of signal for PDGF-BB detection. This DNA walker based assay could detect PDGF-BB down to sub-pM level in 1 h and show good detection accuracy for PDGF-BB secreted by cancer cells. The proposed assay could also be conveniently applied for sensitive detection of other proteins by using corresponding aptamer probes, showing good promise for practical diagnosis.

2. Experiment section

2.1. Materials and apparatus

Human recombinant PDGF-BB was obtained from R&D system (USA). PDGF-AA and PDGF-AB were achieved from Pepro Tech (USA) and BOSTER Biological Technology Co., Ltd. (China), respectively. Thrombin, Gold (III) chloride trihydrate ($HAuCl_4 \cdot 3H_2O$) and tris (hydroxymethyl) aminomethane (Tris) were obtained from Sigma-Aldrich (USA). Trisodium citrate dihydrate was bought from Nanjing Chemical Reagent Co., Ltd. (China). Human PDGF-BB ELISA kit was supplied by MultiSciences Biotech Co., Ltd. (China). Nt.BbvCI and NEB cutsmart buffer were obtained from New England Biolab (USA). Fetal bovine serum (FBS), bovine serum albumin (BSA), RPMI-1640 cell culture medium and trypsin were obtained from KeyGen Biotech Co., Ltd. (China). β-estradiol was obtained from J&K Scientific (China). Carcinoembryonic antigen (CEA), α-fetoprotein (AFP), and carcinoma antigen 125 (CA 125) were purchased from Beijing Keybiotech Co., Ltd. (China). Human serum samples were supplied by Jiangsu Cancer Hospital. Ultrapure water from a Millipore water purification system (Milli-Q, Millipore) was used for the whole experiment. All other reagents were used without further purification. The assay buffer (pH 7.4) contained 10 mM Tris-HCl, 50 mM KCl, 1 mM $MgCl_2$, and 100 μg mL^{-1} BSA. All DNA oligonucleotides were synthesized and purified by Sangon Biotechnology Co., Ltd. (Shanghai, China), and the DNA sequences were listed in Table S1, supplementary.

Hitachi F-7000 fluorescence spectrophotometer (Hitachi, Japan) was used to collect fluorescence signal at room temperature.

2.2. Synthesis of 3D DNA track

13 nm AuNPs were synthesized according to previous report [38]. Briefly, 5 mL of 38.8 mM trisodium citrate was added quickly to 50 mL of 1 mM $HAuCl_4$ boiled in a three-necked flask under robust stirring. After 30 min stirring, the solution was cooled down to room temperature and then stored at 4 °C before usage. The concentration of AuNPs was calculated to 11 nM with the extinction coefficient of 1.39×10^8 M^{-1} cm^{-1} by using the absorbance at 520 nm [39].

The 3D DNA track was constructed by modifying high-density FAM-labeled hairpin DNA1 (FAM-DNA1) on AuNPs (Au-DNA1) [40–42]. Firstly, annealed FAM-DNA1 was mixed with AuNPs at a molar ratio of 300:1, followed by freezing at −20 °C for 2 h. After thawing at room temperature, excess FAM-DNA1 was removed by centrifugation to obtain the Au-DNA1. The obtained Au-DNA1, defined as 3D DNA track, was stored at the concentration of 4 nM in Tris-HCl buffer (pH 7.4) with 0.01% Tween-20 before usage.

To evaluate the number of FAM-DNA1 on each AuNP, 10 mM dithiothreitol (DTT) was added into the Au-DNA1 to replace the FAM-DNA1 from AuNP surfaces [43]. After the overnight incubation at room temperature under stirring, the solution was centrifuged and the fluorescence of supernatant was measured to calculate the amount of FAM-DNA1. Solutions containing DTT and serial concentrations of standard FAM-DNA1 were measured as calibration. The loading number of FAM-DNA1 on each AuNP was then derived.

2.3. Detection of PDGF-BB

A pair of aptamer probes (DNA3 and DNA4) were used as affinity regents for PDGF-BB detection. The mixture of DNA2 and DNA3 with a molar ratio of 1:1.25 was heated at 95 °C for 5 min and cooled slowly to 20 °C over 3 h to form the DNA2/DNA3 duplex (ds-DNA2/3). 20 μL of various concentrations of PDGF-BB was added into 40 μL of the assay buffer containing 20 nM ds-DNA2/3 and DNA4 for a pre-incubation at 37 °C for 20 min, followed by mixing with 20 μL of the mixture of Au-DNA1, $MgCl_2$, and Nt.BbvCI to obtain a total reaction volume of 80 μL, in which the final concentrations of Au-DNA1, $MgCl_2$, and Nt.BbvCI were 0.75 nM, 10 mM, and 0.19 U μL^{-1}, respectively. Here, the Nt.BbvCI was pretreated with 60 mM H_2O_2 before usage for 10 min to oxide DTT in the storage buffer [25]. The mixture solution was then incubated for 1 h at 37 °C and the fluorescence was detected with excitation at 485 nm and emission at 515 nm.

2.4. Detection of PDGF-BB secreted by MCF-7 cell

MCF-7 human breast cancer cells were cultured in 5 mL of RPMI-1640 supplemented with 10% FBS at 37 °C until about 90% confluent (~4.5×10^6 cells in the T-25 flask). Then the MCF-7 cells were cultured for another 32 h in 2.5 mL of serum-free RPMI-1640 with and without 5×10^{-7} M β-estradiol. At certain intervals, 200 μL of supernatant was collected as sample for PDGF-BB detection. Here, the medium was supplemented with fresh RPMI-1640 immediately to maintain the total volume after each sample collection. Following the same detection procedure described above, the PDGF-BB secreted by MCF-7 cells was monitored. Solutions containing serial concentrations of standard PDGF-BB and 25% RPMI-1640 were measured as calibration. As a contrast, samples were also detected with a commercial PDGF-BB ELISA kit.

2.5. Detection of thrombin

For the detection of thrombin, a pair of thrombin aptamers (DNA5 and DNA6) were used for affinity recognition. Firstly, the DNA2/DNA5 duplex (ds-DNA2/5) was prepared under the same operation as ds-DNA2/3. Then, 20 μL of various concentrations of thrombin was added into 60 μL of 1 × cutsmart buffer containing ds-DNA2/5, DNA6, Au-DNA1 and Nt.BbvCI with the final concentrations of 10 nM, 10 nM, 0.75 nM and 0.19 U μL^{-1}, respectively. After a 1-h incubation at 37 °C, the fluorescent spectrum of the solution was recorded.

3. Results and discussion

3.1. Design of the proximity hybridization-induced on particle DNA walker

The proximity hybridization-induced on particle DNA walker system consisted of a pair of aptamer probes (DNA3 and DNA4), a DNA walker (DNA2), a nicking endonuclease (Nt.BbvCI), and the 3D DNA track (Au-DNA1) to perform the target recognition and signal generation (Scheme 1). Here, the DNA2 walker was pre-locked by DNA3 in the form of DNA2/DNA3 duplex (ds-DNA2/3) with 13 complementary bases. In the presence of PDGF-BB, the simultaneous recognition of PDGF-BB with the two aptamer probes brought ds-DNA2/3 and DNA4 into close proximity. As the DNA4 had 11 complementary bases with DNA3, it could perform proximity-assisted displacement of DNA2 to hybridize with DNA3, resulting in the activation of DNA2 walker. Subsequently, the free DNA2 opened the hairpin DNA1 with 11 complementary bases to form a specific recognition site for nicking endonuclease. With the enzymatic cleavage of Nt.BbvCI, a fragment of FAM-DNA1 was detached from the AuNP surface, meanwhile, DNA2 was free again to open another DNA1 nearby. Theoretically, DNA2 could be recycled to traverse the Au-DNA1, leading to the circular release of FAM-DNA1 fragment and hence the amplified fluorescence signal for sensitive detection of PDGF-BB secreted by cancer cells.

3.2. Characterization of the 3D DNA track

In this work, AuNPs with an average diameter of 13 nm were used for functionalization of high-density FAM-DNA1 to construct the 3D DNA track (Fig. 1A). UV/vis absorption, hydration diameters and zeta potentials were measured to evaluate the fabrication of Au-DNA1. Compared with AuNPs, the absorption peak shifted from 520 nm to 525 nm for Au-DNA1 (Fig. 1B). The red-shift of absorption peak indicated the increase of AuNPs diameter by surface modification. Dynamic light scattering measurements also showed obvious increase of the average hydrodynamic diameter from 18 nm of AuNPs to 33 nm of Au-DNA1 (Fig. 1C), suggesting the successful modification of FAM-DNA1 on AuNP surface. In addition, zeta potential analysis showed the Au-DNA1 was less negative than bare AuNP (Fig. 1D), which attributed to the replacement of citrate anions by DNA1 on AuNPs surface [44]. All the above results confirmed the successful fabrication of Au-DNA1 with good dispersity in aqueous media. The coverage of DNA1 on each AuNP could be calculated to be 76 by dissociating FAM-DNA1 from Au-DNA1 and then measuring the concentration of FAM-DNA1 in the supernatant solution and the amount of AuNPs. Thus, the density of DNA1 on AuNPs as well as the intermolecular space could be calculated to be 1.43×10^{13} per cm^2 and 2.6 nm, respectively.

3.3. Feasibility of the DNA walker based assay

Due to the hairpin structure of DNA1, FAM was in near close to the AuNP and the Au-DNA1 showed weak fluorescence. Slight increase of the fluorescence intensity was observed in the coexistence of Au-DNA1 with Nt.BbvCI, ds-DNA2/3, and DNA4 (curves a-c, Fig. 2A). These results indicated DNA2 was well inactivated in the form of ds-DNA2/3 in the absence of PDGF-BB. In presence of PDGF-BB, the fluorescence intensity increased sharply (curve d, Fig. 2A), which indicated the successful activation of DNA2 walker by the proximity hybridization-induced DNA displacement and its walking on Au-DNA1 by enzymatic cleavage, confirming the feasibility of the DNA walker based assay.

On the other hand, the fluorescence signal was unable to be

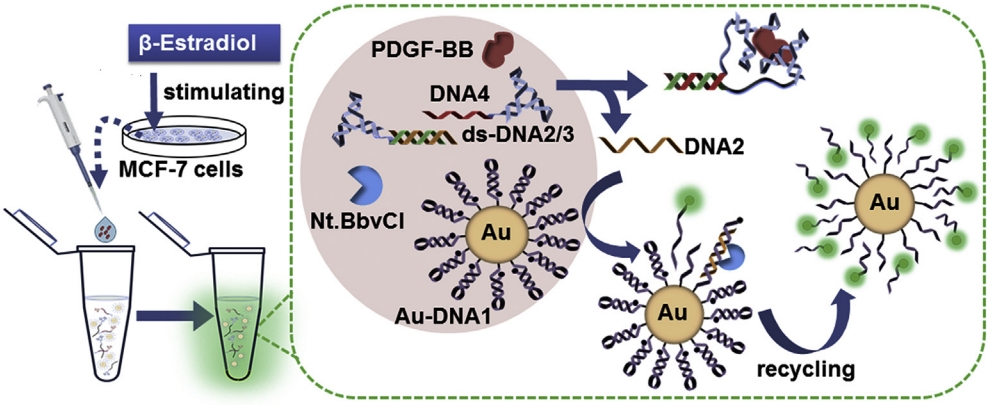

Scheme 1. Schematic illustration of the detection of PDGF-BB secreted by MCF-7 cells using proximity hybridization-induced on particle DNA walker.

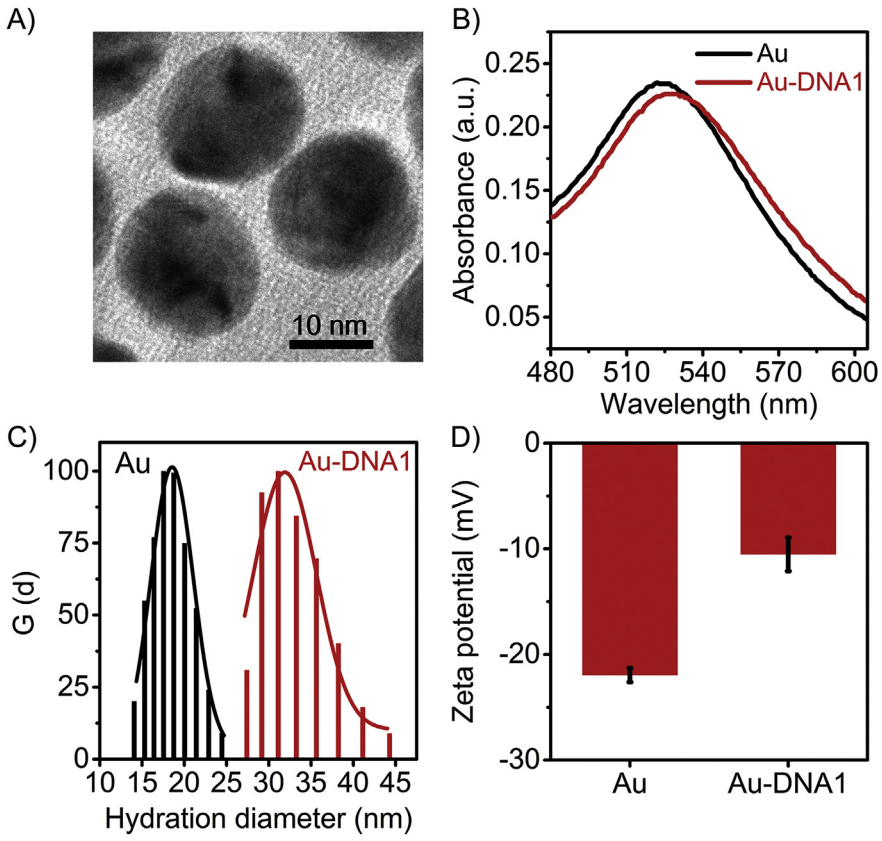

Fig. 1. (A) TEM image of AuNPs. (B) UV–vis spectra, (C) hydration diameters and (D) Zeta potentials of AuNPs and Au-DNA1.

generated only by DNA2 hybridization but without walking via enzymatic cleavage (curve a, Fig. 2B). This was because the formed double strand DNA1/DNA2 had only 11 complementary bases, and could push fluorophore away from the AuNP surface for only 3 nm, which was less than the efficient quenching distance (~10 nm) of AuNP based resonant energy transfer [45]. In the presence of Nt.BbvCI, DNA2 walked on the Au-DNA1 by enzymatic cleavage to produce amplified signal (curve b, Fig. 2B). This on particle DNA walker strategy could detect DNA2 from 0.02 to 300 pM with detection limit down to 13 fM (Fig. S1, supplementary), exhibiting good potential for developing sensitive protein assays by combining with proximity hybridization methods.

The proximity hybridization-induced DNA displacement was further characterized by using a FAM labeled DNA3 (DNA3′) and a Dabcyl labeled DNA2 (DNA2′) (Fig. S2A, supplementary). In the absence of PDGF-BB, DNA2 hybridized stably with DNA3 in the form of ds-DNA2'/3'even in the existence of DNA4, resulting in the approach of FAM to Dabcyl and hence the low fluorescence intensity (curves a and b, Fig. 2C). An obvious increase of the fluorescence intensity was observed in the presence of PDGF-BB (curve c, Fig. 2C), confirming the proximity hybridization-induced DNA displacement.

In comparison to the conventional assay based on proximity hybridization-induced enzymatic hairpin DNA recycling strategy in which FAM/Dabcyl double labeled hairpin DNA1 (DNA1') was used (Fig. S3A, supplementary), the proposed DNA walker based assay showed lower background and higher signal (Fig. 2D) owning to the strong quenching ability of AuNPs, and the high local concentration of DNA tracks on AuNP surface. The good signal to noise ratio (S/N) of the DNA walker based assay also confirmed its high sensitivity for PDGF-BB detection.

3.4. Optimization of assay conditions

The complementary length of DNA3 and DNA4 was the key factor affecting the detection performance of the proposed assay. In the case of high complementary length between DNA3 and DNA4, the two DNA strands could be hybridized without the help of proximity effect, leading to a high background; on the other hand, with short complementary length, the DNA4 was unable to displace DNA2 from ds-DNA2/3 even with the assistance of proximity effect, resulting in a low signal. Considering the 13 complementary bases of ds-DNA2/3, DNA4 with 10–15 complementary bases to DNA3 was used for optimization (Fig. 3A). As expected, the signal as well as the noise increased by increasing the complementary base number of DNA3 and DNA4. Taking consideration of the S/N, a complementary length of 11 bases was chosen in this work.

In addition, the concentration of Au-DNA1, ds-DNA2/3 and DNA4, and the incubation time of enzymatic cleavage was also optimized. With the increase of the concentration of Au-DNA1, the signal increased sharply but the noise increased slowly when the concentration of Au-DNA1 was lower than 1.00 nM (Fig. 3B). Considering the S/N, 0.75 nM of Au-DNA1 was selected. In contrast, the noise was more affected than the signal by increasing the concentration of ds-DNA2/3 and DNA4 (Fig. 3C). Taking into account the detection range of PDGF-BB, 10 nM was chosen for ds-DNA2/3 and DNA4. Fig. 3D showed the signal increased with increasing the incubation time and reached the flat value at the incubation time up to 45 min. In order to ensure complete enzymatic cleavage, 1-h incubation was used in this work.

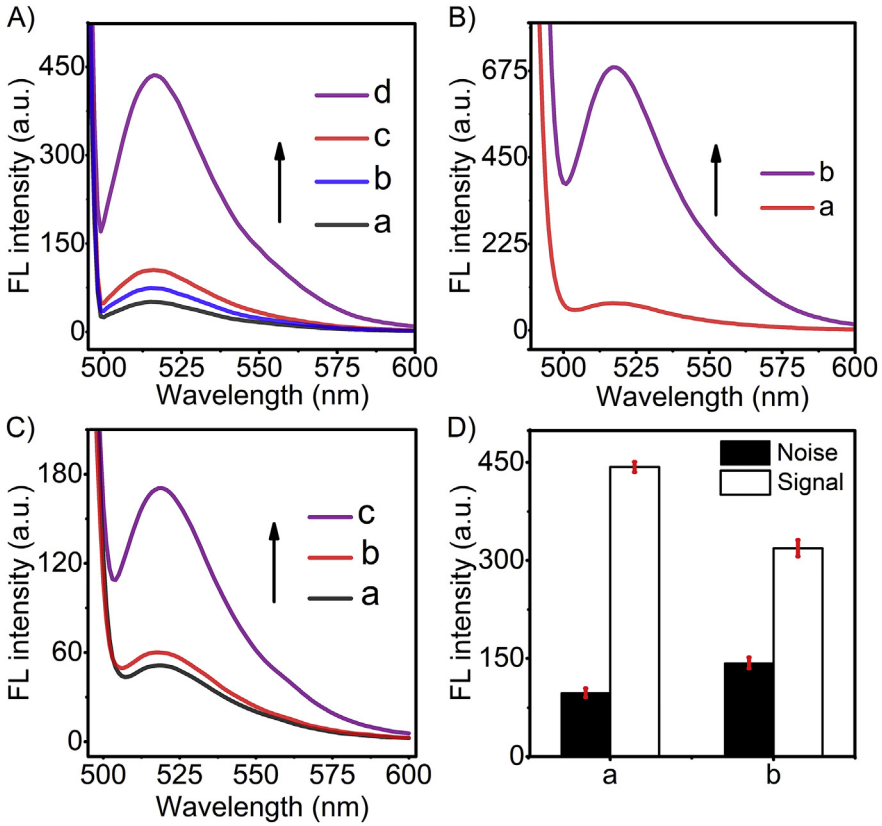

Fig. 2. (A) Fluorescence spectra of (a) Au-DNA1+Nt.BbvCI, (b) (a)+ds-DNA2/3, (c) (b)+DNA4, and (d) (c)+300 pM PDGF-BB. (B) Fluorescence spectra of (a) Au-DNA1+300 pM DNA2, and (b) (a)+ Nt.BbvCI. (C) Fluorescence spectra of (a) 40 nM ds-DNA2′/3′, (b) (a)+40 nM DNA4, (c) (b)+10 nM PDGF-BB. (D) Detection of 300 pM PDGF-BB by (a) the proposed assay and (b) the assay using proximity hybridization-induced enzymatic hairpin DNA recycling.

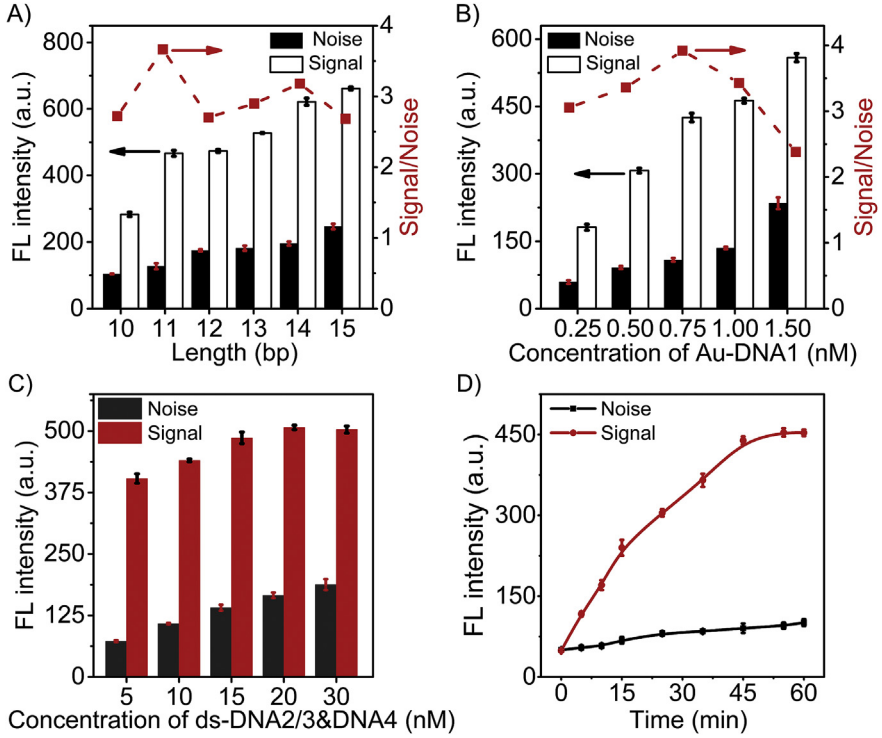

Fig. 3. Optimization of (A) the complementary length between DNA3 and DNA4, (B) concentration of Au-DNA1, (C) concentration of ds-DNA2/3 and DNA4, and (D) incubation time. The concentrations of Au-DNA1, ds-DNA2/3, DNA4, Nt.BbvCI and PDGF-BB were always 0.75 nM, 10 nM, 10 nM, 0.19 U μL^{-1} and 300 pM, respectively, except when it was optimized.

3.5. Assay of PDGF-BB

Under optimal conditions, the fluorescence intensity proportionally increased with increasing PDGF-BB concentration (Fig. 4A). The intensity was log-linear correlation with PDGF-BB concentration in 1–4500 pM with the linear equation of $F = 136 + 115 \lg C_{(pM)}$. The detection limit was calculated to 0.59 pM (15 pg mL^{-1}) corresponding to the signal of blank plus 3 times standard deviation (Fig. 4B). Obviously, the detection limit as well as the detection range was better than the assays based on proximity hybridization-induced DNA displacement (Fig. S2, supplementary) and enzymatic hairpin DNA recycling (Fig. S3, supplementary) which showed detection ranges of 2–25 nM and 0.02–3 nM with detection limits of 0.83 nM and 9.48 pM, respectively. In addition, the detection limit was more than 1000 times lower than the fluorescent assay using binding-induced strand displacement [11], 700 times lower than the endonuclease-assisted circular fluorescent assay [46], and also much lower than the fluorescent assay using a swing arm-based 3D DNA machine [25,37]. The detection performance of this work for PDGF-BB was superior to that of most fluorescent assays using different amplification strategies except PCR, and was also comparable to electrochemical assays (Table S2, supplementary). The high sensitivity of the proposed assay should be attributed both to the enhanced signal from on particle DNA walker based amplification and the low background from the Au-DNA1 in which the fluorescence of FAM-DNA1 could be quenched efficiently by AuNP *via* resonant energy transfer.

One thing to be noted, PDGF-BB at the concentration ranging from 0.1 to 1 pM also could be detected and good linear correlation between the intensity and logarithm of PDGF-BB concentration was obtained (inset, Fig. 4B). However, the detection sensitivity (the slope of the linear equation) of PDGF-BB ranging from 0.1 to 1 pM was much lower than that of PDGF-BB ranging from 1 to 4500 pM. Thus, for preciseness, the proposed assay could apply for qualitative detection of PDGF-BB in 0.1–1 pM.

The specificity of the proposed assay was evaluated by applying this assay to detect solutions containing CEA, BSA, CA 125, thrombin, PDGF-AA, PDGF-AB and PDGF-BB (Fig. 4C). Except PDGF-BB, no signal was observed for CEA, BSA, CA 125 and thrombin. In addition, for PDGF-AA and PDGF-AB, the other two members in PDGF family with structures similar to PDGF-BB, only slight signal was observed. This should be due to the sandwich recognition format and the low binding affinity of PDGF-BB aptamer to PDGF-A part in PDGF-AA and PDGF-AB [8]. These results demonstrated the good specificity of the assay.

As the concentration of PDGF-BB was sub-nM in cancer human serum samples [47] and 8–40 pM in plasma [48], the proposed assay offering the detection range of 1–4500 pM could detect PDGF-BB in serum sample for cancer diagnosis. The recovery test of the proposed assay was conducted in diluted human serum samples (Table 1). The relative standard deviations (RSD) were lower than 9%, revealing the good accuracy of the proposed assay.

The practical application of the DNA walker based assay was evaluated by monitoring the PDGF-BB secreted by MCF-7 human breast cancer cells [49]. The concentrations of PDGF-BB from both stimulated and unstimulated groups were tested by the DNA walker based assay and commercial ELISA method (Fig. 5). During the 24 h culture, PDGF-BB at pM level was secreted by MCF-7 cells and the concentration of PDGF-BB increased gradually in both cases of stimulation and non-stimulation. Obviously, MCF-7 cells with β-estradiol stimulation secreted higher level of PDGF-BB (Fig. 5B). However, after 32 h culture in serum-free medium, MCF-7 cells lost their integrality and the supernatant turned turbid, leading to the decrease of the concentration of PDGF-BB. These results were consistent with the secretion of PDGF-BB reported in the literatures [50,51]. In addition, the concentration value of PDGF-BB as well as its changing trend during MCF-7 cells culture was similar to that from the commercial ELISA method, revealing the good reliability of the proposed assay.

3.6. Detection of thrombin

The DNA walker based assay could be easily extended to detect other proteins by using corresponding aptamer probes. Here, by using a pair of thrombin aptamer probes (DNA5 and DNA6), the DNA walker based assay was also used for sensitive detection of thrombin. Similar to the detection of PDGF-BB, the simultaneous recognition of thrombin by DNA5 and DNA6 induced the proximity-assisted DNA displacement to free DNA2 walker, which subsequently walked on Au-DNA1 by enzymatic cleavage to release FAM-DNA1 fragment and generate amplified fluorescent signal (Fig. 6A). Here the reaction time were also optimized to be 1 h

Table 1
Recovery results of PDGF-BB in diluted serum samples.

Samples (pM)	Added (pM)	Found (pM)	Recovery (%)	RSD[a] (%)
1	3	3.22	107.23	8.41
2	30	30.33	101.09	4.01
3	300	274.03	91.34	5.61
4	1000	960.23	96.02	3.17

[a] Means three parallel experiments.

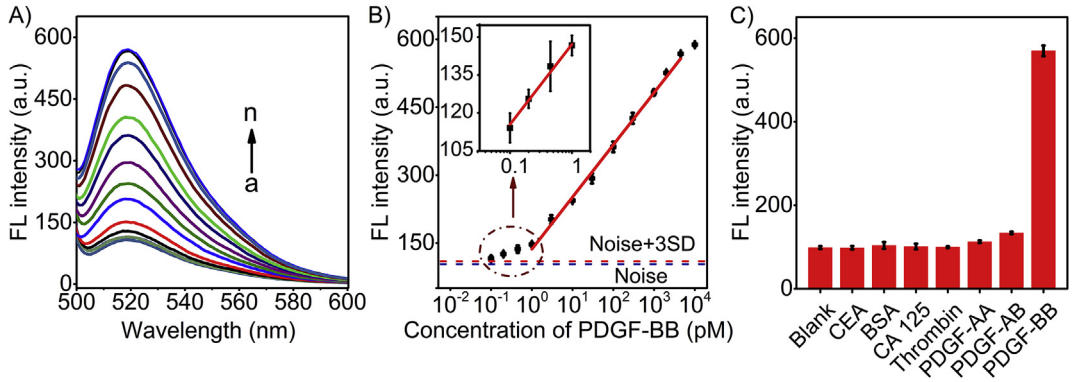

Fig. 4. (A) Fluorescence spectra of the DNA walker based assay of PDGF-BB with concentrations at (from a to n) 0, 0.1, 0.2, 0.45, 1, 3, 10, 30, 100, 300, 1000, 2000, 4500 and 10000 pM. (B) Plot of fluorescence intensity *vs.* logarithm of PDGF-BB concentration. (C) Selectivity evaluation of the assay to 10 nM CEA, 200 μg mL^{-1} BSA, 25 μg mL^{-1} CA125, 10 nM thrombin, 1 nM PDGF-AA, 1 nM PDGF-AB and 1 nM PDGF-BB.

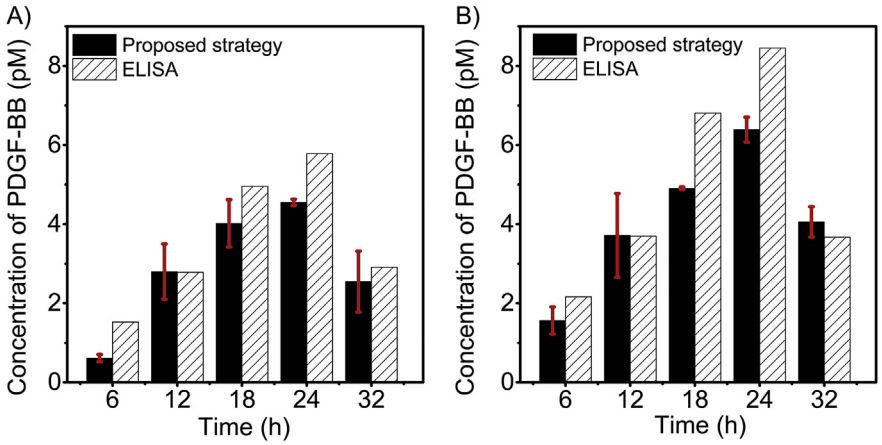

Fig. 5. Measurement of PDGF-BB secreted by MCF-7 cells without (A) and with (B) β-estradiol stimulation after certain intervals by both the DNA walker based assay and commercial ELISA.

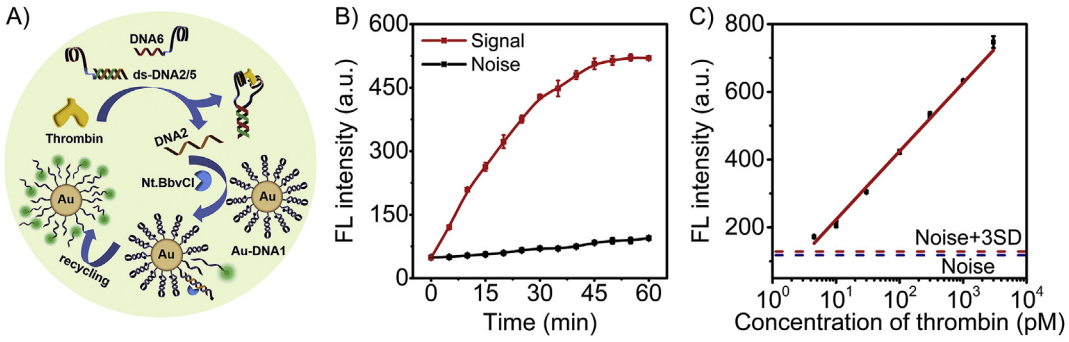

Fig. 6. (A) Illustration of thrombin detection by the proximity hybridization-induced on particle DNA walker. (B) Optimization of the assay time of thrombin. (C) Plot of fluorescence intensity *vs.* logarithm of thrombin concentration.

(Fig. 6B). The linear range for thrombin detection was from 4.5 to 3000 pM with a detection limit of 3.43 pM (Fig. 6C).

4. Conclusion

A proximity hybridization-induced on particle DNA walker has been developed for simple and sensitive detection of PDGF-BB. The proximity binding of PDGF-BB with two aptamer probes induces the activation of the DNA walker and subsequent the movement on the 3D tracks to circularly generate fluorescent signal. Benefiting from the DNA walker based signal amplification, the assay can detect PDGF-BB sensitively down to sub-pM level. Additionally, the assay can reliably monitor the secretion of PDGF-BB from cancer cells with stimulation. By adopting the specific aptamer probes, the assay is also able to detect other proteins sensitively. The proposed assay with the tandem design of proximity hybridization-induced DNA displacement and 3D DNA walker possesses advantages of simplicity, high sensitivity and selectivity, and good practical applicability and extensibility, showing promise for practical diagnosis.

Declarations of interest

None.

Acknowledgements

We gratefully thank the National Natural Science Foundation of China (21575063 and 21827812), and Independent Research Foundation from State Key Laboratory of Analytical Chemistry for Life Science (5431ZZXM1807) for funding supply.

Appendix A. Supplementary data

Supplementary data to this article can be found online at https://doi.org/10.1016/j.aca.2019.05.013.

References

[1] C.H. Heldin, B. Westermark, Mechanism of action and in vivo role of platelet-derived growth factor, Physiol. Rev. 79 (1999) 1283–1316.
[2] C.H. Heldin, Targeting the PDGF signaling pathway in tumor treatment, Cell Commun. Signal. 11 (2013) 97.
[3] K. Appiah-Kubi, Y. Wang, H. Qian, M. Wu, X.Y. Yao, Y. Wu, Y.C. Chen, Platelet-derived growth factor receptor/platelet-derived growth factor (PDGFR/PDGF) system is a prognostic and treatment response biomarker with multifarious therapeutic targets in cancers, Tumor Biol. 37 (2016) 10053–10066.
[4] X. Salcedo, J. Medina, P. Sanz-Cameno, L. Garcia-Buey, S. Martin-Vilchez, R. Moreno-Otero, Review article: angiogenesis soluble factors as liver disease markers, Aliment, Pharmacol. Ther. 22 (2005) 23–30.
[5] S.Y. Chun, G.J. Lim, T.G. Kwon, E.K. Kwak, B.W. Kim, A. Atala, J.J. Yoo, Identification and characterization of bioactive factors in bladder submucosa matrix, Biomaterials 28 (2007) 4251–4256.
[6] F. Perros, D. Montani, P. Dorfmuller, I. Durand-Gasselin, C. Tcherakian, J. Le Pavec, M. Mazmanian, E. Fadel, S. Mussot, O. Mercier, P. Herve, D. Emilie, S. Eddahibi, G. Simonneau, R. Souza, M. Humbert, Platelet-derived growth factor expression and function in idiopathic pulmonary arterial hypertension, Am. J. Respir. Crit. Care Med. 178 (2008) 81–88.
[7] N. Razmi, B. Baradaran, M. Hejazi, M. Hasanzadeh, J. Mosafer, A. Mokhtarzadeh, M. de la Guardia, Recent advances on aptamer-based biosensors to detection of platelet-derived growth factor, Biosens. Bioelectron. 113 (2018) 58–71.

[8] L.S. Green, D. Jellinek, R. Jenison, A. Ostman, C.H. Heldin, N. Janjic, Inhibitory DNA ligands to platelet-derived growth factor B-chain, Biochemistry 35 (1996) 14413–14424.
[9] C.J. Yang, S. Jockusch, M. Vicens, N.J. Turro, W.H. Tan, Light-switching excimer probes for rapid protein monitoring in complex biological fluids, Proc. Natl. Acad. Sci. U.S.A. 102 (2005) 17278–17283.
[10] J.J. Liu, X.R. Song, Y.W. Wang, A.X. Zheng, G.N. Chen, H.H. Yang, Label-free and fluorescence turn-on aptasensor for protein detection via target-induced silver nanoclusters formation, Anal. Chim. Acta 749 (2012) 70–74.
[11] F. Li, H.Q. Zhang, C. Lai, X.F. Li, X.C. Le, A molecular translator that acts by binding-induced DNA strand displacement for a homogeneous protein assay, Angew. Chem. Int. Ed. 51 (2012) 9317–9320.
[12] R.Y. Lai, K.W. Plaxco, A.J. Heeger, Aptamer-based electrochemical detection of picomolar platelet-derived growth factor directly in blood serum, Anal. Chem. 79 (2007) 229–233.
[13] D.B. Zhu, X.M. Zhou, D. Xing, A new kind of aptamer-based immunomagnetic electrochemiluminescence assay for quantitative detection of protein, Biosens. Bioelectron. 26 (2010) 285–288.
[14] C.C. Huang, Y.F. Huang, Z.H. Cao, W.H. Tan, H.T. Chang, Aptamer-modified gold nanoparticles for colorimetric determination of platelet-derived growth factors and their receptors, Anal. Chem. 77 (2005) 5735–5741.
[15] H. Li, Y. Zhu, S.Y. Dong, W.B. Qiang, L. Sun, D.K. Xu, Fast functionalization of silver decahedral nanoparticles with aptamers for colorimetric detection of human platelet-derived growth factor-BB, Anal. Chim. Acta 829 (2014) 48–53.
[16] Y.X. Jiang, X.H. Fang, C.L. Bai, Signaling aptamer/protein binding by a molecular light switch complex, Anal. Chem. 76 (2004) 5230–5235.
[17] H.Q. Zhang, F. Li, B. Dever, C. Wang, X.F. Li, X.C. Le, Assembling DNA through affinity binding to achieve ultrasensitive protein detection, Angew. Chem. Int. Ed. 52 (2013) 10698–10705.
[18] H.Q. Zhang, F. Li, B. Dever, X.F. Li, X.C. Le, DNA-mediated homogeneous binding assays for nucleic acids and proteins, Chem. Rev. 113 (2013) 2812–2841.
[19] M. Lundberg, A. Eriksson, B. Tran, E. Assarsson, S. Fredriksson, Homogeneous antibody-based proximity extension assays provide sensitive and specific detection of low-abundant proteins in human blood, Nucleic Acids Res. 39 (2011) e102.
[20] M. Gullberg, S.M. Gustafsdottir, E. Schallmeiner, J. Jarvius, M. Bjarnegard, C. Betsholtz, U. Landegren, S. Fredriksson, Cytokine detection by antibody-based proximity ligation, Proc. Natl. Acad. Sci. U.S.A. 101 (2004) 8420–8424.
[21] C. Zong, J. Wu, M.M. Liu, F. Yan, H.X. Ju, High-throughput imaging assay of multiple proteins via target-induced DNA assembly and cleavage, Chem. Sci. 6 (2015) 2602–2607.
[22] Q. Xiao, J. Wu, P. Dang, H.X. Ju, Multiplexed chemiluminescence imaging assay of protein biomarkers using DNA microarray with proximity binding-induced hybridization chain reaction amplification, Anal. Chim. Acta 1032 (2018) 130–137.
[23] J. Zhu, H.Y. Gan, J. Wu, H.X. Ju, Molecular machine powered surface programmatic chain reaction for highly sensitive electrochemical detection of protein, Anal. Chem. 90 (2018) 5503–5508.
[24] F. Li, H.Q. Zhang, Z.X. Wang, X.K. Li, X.F. Li, X.C. Le, Dynamic DNA assemblies mediated by binding-induced DNA strand displacement, J. Am. Chem. Soc. 135 (2013) 2443–2446.
[25] H.Q. Zhang, M.D. Lai, A. Zuehlke, H.Y. Peng, X.F. Li, X.C. Le, Binding-induced DNA nanomachines triggered by proteins and nucleic acids, Angew. Chem. Int. Ed. 54 (2015) 14326–14330.
[26] X.M. Qu, D. Zhu, G.B. Yao, S. Su, J. Chao, H.J. Liu, X.L. Zuo, L.H. Wang, J.Y. Shi, L.H. Wang, W. Huang, H. Pei, C.H. Fan, An exonuclease III-powered, on-particle stochastic DNA walker, Angew. Chem. Int. Ed. 56 (2017) 1855–1858.
[27] W. Wei, M. Wei, L.H. Yin, Y.P. Pu, S.Q. Liu, Improving the fluorometric determination of the cancer biomarker 8-hydroxy-2'-deoxyguanosine by using a 3D DNA nanomachine, Microchim. Acta 185 (2018) 494–500.
[28] P.X. Li, M. Wei, F. Zhang, J. Su, W. Wei, Y.J. Zhang, S.Q. Liu, Novel fluorescence switch for microRNA imaging in living cells based on DNAzyme amplification strategy, ACS Appl. Mater. Interfaces 10 (2018) 43405–43410.
[29] M. Wei, C.L. Wang, E.S. Xu, J. Chen, X.L. Xu, W. Wei, S.Q. Liu, A simple and sensitive electrochemiluminescence aptasensor for determination of ochratoxin A based on a nicking endonuclease-powered DNA walking machine, Food Chem. 282 (2019) 141–146.
[30] C.P. Liang, P.Q. Ma, H. Liu, X.G. Guo, B.C. Yin, B.C. Ye, Rational engineering of a dynamic, entropy-driven DNA nanomachine for intracellular microRNA imaging, Angew. Chem. Int. Ed. 56 (2017) 9077–9081.
[31] C. Jung, P.B. Allen, A.D. Ellington, A stochastic DNA walker that traverses a microparticle surface, Nat. Nanotechnol. 11 (2016) 157–163.
[32] Y. Zhang, L.X. Wang, F. Luo, B. Qiu, L.H. Guo, Z.Q. Weng, Z.Y. Lina, G.N. Chen, An electrochemiluminescence biosensor for Kras mutations based on locked nucleic acid functionalized DNA walkers and hyperbranched rolling circle amplification, Chem. Commun. 53 (2017) 2910–2913.
[33] M.Q. He, K. Wang, W.J. Wang, Y.L. Yu, J.H. Wang, Smart DNA machine for carcinoembryonic antigen detection by exonuclease III-assisted target recycling and DNA walker cascade amplification, Anal. Chem. 89 (2017) 9292–9298.
[34] K. Yang, H. Wang, N. Ma, M. Zeng, H. Luo, D. He, A programmable target-initiated DNAzyme walker walking along a spatially isolated and highly hybridizable substrate track on nanoparticle surface, ACS Appl. Mater. Interfaces 10 (2018) 37386–37395.
[35] Z.Q. Xu, P. Zhang, Y.Q. Chai, H.J. Wang, R. Yuan, A biosensor based on a 3D-DNA walking machine network and distance-controlled electrochemiluminescence energy transfer for ultrasensitive detection of tenascin C and lead ions, Chem. Commun. 54 (2018) 8741–8744.
[36] P.Q. Ma, C.P. Liang, H.H. Zhang, B.C. Yin, B.C. Ye, A highly integrated DNA nanomachine operating in living cells powered by an endogenous stimulus, Chem. Sci. 9 (2018) 3299–3304.
[37] F. Li, Y. Lin, A. Lau, Y. Tang, J. Chen, X.C. Le, Binding-induced molecular amplifier as a universal detection platform for biomolecules and biomolecular interaction, Anal. Chem. 90 (2018) 8651–8657.
[38] J. Liu, Y. Lu, Preparation of aptamer-linked gold nanoparticle purple aggregates for colorimetric sensing of analytes, Nat. Protoc. 1 (2006) 246–252.
[39] W. Haiss, N.T.K. Thanh, J. Aveyard, D.G. Fernig, Determination of size and concentration of gold nanoparticles from UV-Vis spectra, Anal. Chem. 79 (2007) 4215–4221.
[40] B.W. Liu, J.W. Liu, Freezing directed construction of bio/nano interfaces: reagentless conjugation, denser spherical nucleic acids, and better nanoflares, J. Am. Chem. Soc. 139 (2017) 9471–9474.
[41] B. Liu, J.W. Liu, Methods for preparing DNA-functionalized gold nanoparticles, a key reagent of bioanalytical chemistry, Anal. Methods 9 (2017) 2633–2643.
[42] X. Zhang, T. Gouriye, K. Goeken, M.R. Servos, R. Gill, J.W. Liu, Toward fast and quantitative modification of large gold nanoparticles by thiolated DNA: scaling of nanoscale forces, kinetics, and the need for thiol reduction, J. Phys. Chem. C 117 (2013) 15677–15684.
[43] H.D. Hill, C.A. Mirkin, The bio-barcode assay for the detection of protein and nucleic acid targets using DTT-induced ligand exchange, Nat. Protoc. 1 (2006) 324–336.
[44] W.J. Wang, X.F. Ding, Q. Xu, J. Wang, L. Wang, X.H. Lou, Zeta-potential data reliability of gold nanoparticle biomolecular conjugates and its application in sensitive quantification of surface absorbed protein, Colloids Surf., B 148 (2016) 541–548.
[45] R. Chhabra, J. Sharma, H.N. Wang, S.L. Zou, S. Lin, H. Yan, S. Lindsay, Y. Liu, Distance-dependent interactions between gold nanoparticles and fluorescent molecules with DNA as tunable spacers, Nanotechnology 20 (2009) 485201.
[46] L.P. Qiu, Z.S. Wu, G.L. Shen, R.Q. Yu, Highly sensitive and selective bifunctional oligonucleotide probe for homogeneous parallel fluorescence detection of protein and nucleotide sequence, Anal. Chem. 83 (2011) 3050–3057.
[47] K. Leitzel, W. Bryce, J. Tomita, G. Manderino, I. Tribby, A. Thomason, M. Billingsley, E. Podczaski, H. Harvey, M. Bartholomew, A. Lipton, Elevated plasma platelet-derived growth factor B-chain levels in cancer-patients, Cancer Res. 51 (1991) 4149–4154.
[48] X.H. Fang, Z.H. Cao, T. Beck, W.H. Tan, Molecular aptamer for real-time oncoprotein platelet-derived growth factor monitoring by fluorescence anisotropy, Anal. Chem. 73 (2001) 5752–5757.
[49] M.D. Coltrera, J. Wang, P.L. Porter, A.M. Gown, Expression of platelet-derived growth factor B-chain and the platelet-derived growth factor receptor β subunit in human breast tissue and breast carcinoma, Cancer Res. 55 (1995) 2703–2708.
[50] D.A. Bronzert, P. Pantazis, H.N. Antoniades, A. Kasid, N. Davidson, R.B. Dickson, M.E. Lippman, Synthesis and secretion of platelet-derived growth factor by human breast cancer cell lines, Proc. Natl. Acad. Sci. U.S.A. 84 (1987) 5763–5767.
[51] B. Yi, P.J. Williams, M. Niewolna, Y. Wang, T. Yoneda, Tumor-derived platelet-derived growth factor-BB plays a critical role in osteosclerotic bone metastasis in an animal model of human breast cancer, Cancer Res. 62 (2002) 917–923.